Ecotoxicology and Environmental Safety 304 (2025) 119095

Contents lists available at ScienceDirect

Ecotoxicology and Environmental Safety

journal homepage: www.elsevier.com/locate/ecoenv

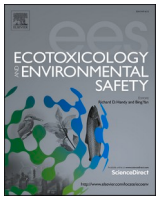

Assessing cardiac insufficiency risks of aflatoxin B1 through network toxicology and molecular docking analyses

Qianyao Zhang [a,1], Qing Zhang [b,1], Piqiao Jiang [c], Xiaotong Zhao [a], Zhonghua Wen [c], Yangyang Liu [d,**,2], Qian Cao [a,**,2], Siyao Wang [d,*,2]

[a] Department of cardiology, Shengjing Hospital of China Medical University, Shenyang, Liaoning 110000, China
[b] Endoscopy Center, The 10th People's Hospital of Shenyang, Shenyang, Liaoning 110000, China
[c] Department of cardiology, Tie Mei General Hospital of Liaoning Health Industry Group, Shenyang, Liaoning 112700, China
[d] School of Public Health, Shenyang Medical College, Shenyang, Liaoning 110034, China

ARTICLE INFO

Keywords:
AFB1
Cardiac insufficiency
Network toxicology
Molecular docking
Molecular dynamics

ABSTRACT

This study aimed to elucidate the promoting effect of Aflatoxin B1 (AFB1) on cardiac insufficiency and its specific molecular mechanisms through methods including network toxicology, molecular docking, dynamics simulation, and in vivo experiments. A total of 44 overlapping targets between cardiac insufficiency and AFB1 toxicity were identified. Subsequently, a PPI network was constructed using STRING and Cytoscape software, and 12 core genes were identified, including AKT1, HIF1A, MMP9, PIK3CA, NFKB1, GSK3B, TLR4, KDR, JAK2, MAPK1, PIK3R1, and PTPN11. GO and KEGG enrichment analyses demonstrated that AFB1-induced cardiac insufficiency is primarily linked to the activation of the PI3K-AKT and MAPK signaling pathways. Molecular docking results showed that AFB1 exhibited strong binding affinity with all 12 core targets, among which its binding ability to JAK2, GSK3B, and MMP9 ranked as the top three. Molecular dynamics simulations focused on the complex formed between AFB1 and JAK2, confirming its favorable stability. Additional murine experiments confirmed that AFB1 exposure induces cardiac insufficiency and activates the PI3K-AKT and MAPK signaling pathways. These findings collectively demonstrate that AFB1 binding to JAK2 activates both the PI3K-AKT and MAPK pathways, consequently promoting cardiac insufficiency. By elucidating the underlying molecular mechanisms, this study establishes a theoretical framework for understanding how chronic AFB1 exposure aggravates cardiac insufficiency.

1. Introduction

Aflatoxins are among the most significant mycotoxins of concern to human health and are primarily produced by *Aspergillus flavus* and *Aspergillus parasiticus* (Claeys et al., 2020). Of the more than 20 identified aflatoxin variants, aflatoxin B1 (AFB1) has been classified as a Group 1 carcinogen by the International Agency for Research on Cancer (IARC) of the World Health Organization (WHO) (Claeys et al., 2020; Rushing and Selim, 2019). AFB1 is well-established for its hepatotoxic effects. Chronic exposure to AFB1 contributes to the development of liver injury, liver cirrhosis and hepatocellular carcinoma (Altyar et al., 2023; Cao et al., 2022). Numerous in vivo studies have demonstrated that the hepatotoxicity of AFB1 primarily arises from two mechanisms: the activation of hepatic cytochrome P450 enzymes (Meijer et al., 2019) and the promotion of excessive reactive oxygen species production, both of which result in hepatocyte damage (Dai et al., 2022; Zhou et al., 2019). In recent years, reports of AFB1 toxicity affecting organs beyond the liver have increased. AFB1 has been shown to promote the development of Alzheimer's disease by inducing DNA damage, oxidative stress, and endoplasmic reticulum stress, thereby impairing DNA repair mechanisms. (Ranjbar et al., 2025). Additionally, AFB1 exacerbates inflammatory responses through disruption of the gut microbiota,

* Correspondence to: School of Public Health, Shenyang Medical College, No.146 Huanghe North Street, Yuhong District, Shenyang City 110034, PR China.
** Corresponding authors.
E-mail addresses: zhangqy0206@163.com (Q. Zhang), zhangqing_76@163.com (Q. Zhang), Jiangpiqiao99@163.com (P. Jiang), zhaoxiaotong9508@163.com (X. Zhao), 386333615@qq.com (Z. Wen), juanjuanmao11@163.com (Y. Liu), cqdoc@163.com (Q. Cao), wangsiyao2021@symc.edu.cn (S. Wang).
[1] Qianyao Zhang and Qing Zhang are co-first authors and they have contributed equally to this work.
[2] Siyao Wang, Qian Cao and Yangyang Liu are co-corresponding authors and they have contributed equally to this work.

https://doi.org/10.1016/j.ecoenv.2025.119095
Received 18 June 2025; Received in revised form 5 September 2025; Accepted 19 September 2025
Available online 26 September 2025

leading to testicular damage and impaired reproductive function (Sabahi et al., 2024; Yan et al., 2025). However, studies investigating AFB1-induced cardiotoxicity remain scarce. A rat study demonstrated that continuous exposure to AFB1 for 14 days significantly elevated cardiac injury (Albadrani et al., 2024). Studies have demonstrated that AFB1 exposure is associated with apoptotic cell death in cardiomyocytes, the infiltration of inflammatory factors, and a rise in lipid peroxidation within cardiac tissue. (Ge et al., 2017; Khalil et al., 2024).

Cardiac insufficiency, clinically referred to as heart failure, is an end-stage impairment of the heart's pumping function caused by multiple factors, such as myocardial infarction, hypertension, and cardiomyopathy. Cardiac fibrosis, characterized by the activation of cardiac fibroblasts and increased synthesis of extracellular matrix following the loss of cardiomyocytes, is a key pathological mechanism in heart failure (Chen et al., 2025). Although initially beneficial for cardiac tissue repair, excessive activation of fibroblasts can lead to adverse ventricular remodeling (Chen et al., 2025; van den Borne et al., 2010). However, the role of AFB1 in cardiac insufficiency has not yet been reported. Therefore, it is particularly important to systematically evaluate its toxicological effects, especially those on the heart. This study aims to investigate the effects of AFB1 on cardiac insufficiency using network toxicology, molecular docking, molecular dynamics simulations, and in vivo experiments. By identifying protein targets and biochemical pathways associated with AFB1 exposure, we seek to elucidate its toxicological mechanisms at the molecular level.

2. Methods

2.1. Acquisition of targets for AFB1 and cardiac insufficiency

The potential targets of AFB1 were predicted using two natural compound target prediction platforms: SuperPred (https://prediction.charite.de/) and Swiss Target Prediction (http://www.swisstargetprediction.ch/). Targets associated with cardiac insufficiency were retrieved from the GeneCards database (https://www.genecards.org/) and the OMIM database (https://omim.org/) for further network analysis. The academic version of Origin 2023 was then used to identify the common targets between AFB1 and cardiac insufficiency, yielding potential targets through which AFB1 may contribute to cardiac insufficiency.

2.2. Construction of the protein-protein interaction (PPI) network

The intersection targets were analyzed using the STRING database to construct a PPI network, with Homo sapiens specified as the organism and a minimum interaction score threshold of 0.400. The resulting PPI network was then imported into Cytoscape 3.9.0 for visualization. Network topology analysis was conducted using the CytoHubba plugin to identify the core targets.

2.3. Gene ontology (GO) and kyoto encyclopedia of genes and genomes (KEGG) enrichment analysis

GO and KEGG enrichment analyses of the overlapping targets between AFB1 exposure and cardiac insufficiency were performed using R version 4.2.2 with the clusterProfiler bioinformatics package. GO functional annotation-covering Biological Process, Cellular Component, and Molecular Function categories-and KEGG pathway enrichment analysis were conducted. Visualization of the GO and KEGG results was achieved through bar plots and bubble charts based on the number of enriched genes, and core signaling pathway diagrams were subsequently generated.

2.4. Molecular docking

Three-dimensional protein structures were retrieved from the Protein Data Bank (PDB) and prepared using PyMOL version 2.3.0. The 3D structure of the ligand, AFB1, was obtained from the PubChem database and energetically minimized to its lowest energy conformation using the MMFF94 force field in OpenBabel version 3.1.1. Protein structures were processed with AutoDock Tools version 1.5.6 to add hydrogen atoms, and the ligand was similarly treated by adding hydrogens and identifying rotatable bonds. Docking parameters were set using the Grid panel in AutoDock Tools: the docking mode was set to semi-flexible (protein rigid, ligand flexible), exhaustiveness was set to 25, and the Lamarckian genetic algorithm was selected. Molecular docking simulations were performed using AutoDock Vina version 1.2.0 to calculate binding affinities. The docking results were visualized with PyMOL version 2.3.0.

2.5. Molecular dynamics simulation

Molecular dynamics simulation of the JAK2 protein - AFB1 complex was performed using Gromacs 2024.4. Amber14sb was selected as the protein force field, and Gaff2 was chosen for the ligand. The TIP4P water model was used to solvate the protein-ligand system, and a periodic boundary water box with a distance of 1.2 nm was created. The Particle Mesh Ewald (PME) method was utilized to calculate long-range electrostatic interactions, and the Monte Carlo ion placement method was used to introduce an appropriate number of sodium and chloride ions to neutralize the entire system. Before the production simulation, system energy minimization and equilibration were performed in three steps:

(1) Each system underwent energy minimization using the steepest descent algorithm for 50,000 steps (stop minimization when the maximum force < 1000 kJ/mol).
(2) With the number of particles, volume, and temperature (310 K) kept constant, each system was pre-equilibrated for 50,000 steps with a time step of 2 fs (NVT ensemble).
(3) With the number of particles, pressure (1 atm), and temperature (310 K) held constant, the system was further pre-equilibrated for 50,000 steps with a time step of 2 fs (NPT ensemble). After energy minimization and equilibration, a 100 ns molecular dynamics simulation was conducted without any restraints, using a 2 fs time step and saving structural coordinates every 10 ps.We analyzed the molecular dynamics simulation trajectories of the JAK2 protein-Aflatoxin B1 complex for root mean square deviation (RMSD), root mean square fluctuation (RMSF), radius of gyration (Rg), the number of hydrogen bonds between the protein and ligand, the distribution of relative free energy, and compared the complex structures at 0, 25, 50, 75, and 100 ns. In addition, the MM/GBSA method was used to calculate the average binding free energy between the protein and the ligand.

2.6. Animal models

All in vivo experiments were approved by the Animal Ethics Committee of Shengjing Hospital, China Medical University. Male C57BL/6 mice (8–10 weeks old) were housed in an SPF-grade facility under a 12-hour light/dark cycle, with six mice per cage and ad libitum access to food and water. Aflatoxin B1 (AFB1) was formulated in polyethylene glycol 300 (PEG 300) containing 1 % dimethyl sulfoxide (DMSO, v/v). Mice received AFB1 at 0.1 mg/kg/day by oral gavage for 6 weeks (total volume 100 μL). The vehicle control group was administered an equivalent volume of the vehicle (1 % DMSO in PEG 300) on the same schedule, matched for dosing frequency and volume. After six weeks of continuous treatment, cardiac tissues were harvested for analysis.

2.7. H&E and masson staining

Cardiac tissue samples were fixed in 4 % paraformaldehyde for 48 h, paraffin-embedded, and sectioned at 5 μm thickness. Sections were

stained with hematoxylin and eosin (H&E) or Masson's trichrome (Servicebio, Wuhan, China) to evaluate the extent of cardiac injury and fibrosis.

commercial reverse transcription kit. Quantitative real-time PCR was carried out with Novastar SYBR qPCR SuperMix. Each experiment included three independent biological replicates, and each sample was analyzed in technical triplicate. The primer sequences are as follows:

Target	Species	Forward (5′–3′)	Reverse (5′–3′)
GAPDH	Mouse	GGAGCGAGATCCCTCCAAAAT	GGCTGTTGTCATACTTCTCATGG
Bnp	Mouse	TCCTCTGGGAAGTCCTAGCC	AGCTGTCTCTGGGCCATTTC
Acta2	Mouse	GGCATCCACGAAACCACCTA	AATGCCTGGGTACATGGTGG
Col1a1	Mouse	CCCAGTGGCGGTTATGACTT	CTCAAGGTCACGGTCACGAA
Tgf-β	Mouse	AGGAGACGGAATACAGGGCT	GGATCCACTTCCAACCCAGG
Tnf-α	Mouse	ATGGCCTCCCTCTCATCAGT	AAGGTACAACCCATCGGCTG
Il−6	Mouse	GCCTTCTTGGGACTGATGCT	AGCCTCCGACTTGTGAAGTG

2.8. Quantitative real-time PCR

Total RNA was extracted from mouse cardiac tissue using the TRIzol method and subsequently reverse transcribed into cDNA using a

2.9. Western blot

Total protein was extracted from murine cardiac tissue and separated by sodium dodecyl sulfate-polyacrylamide gel electrophoresis (SDS-

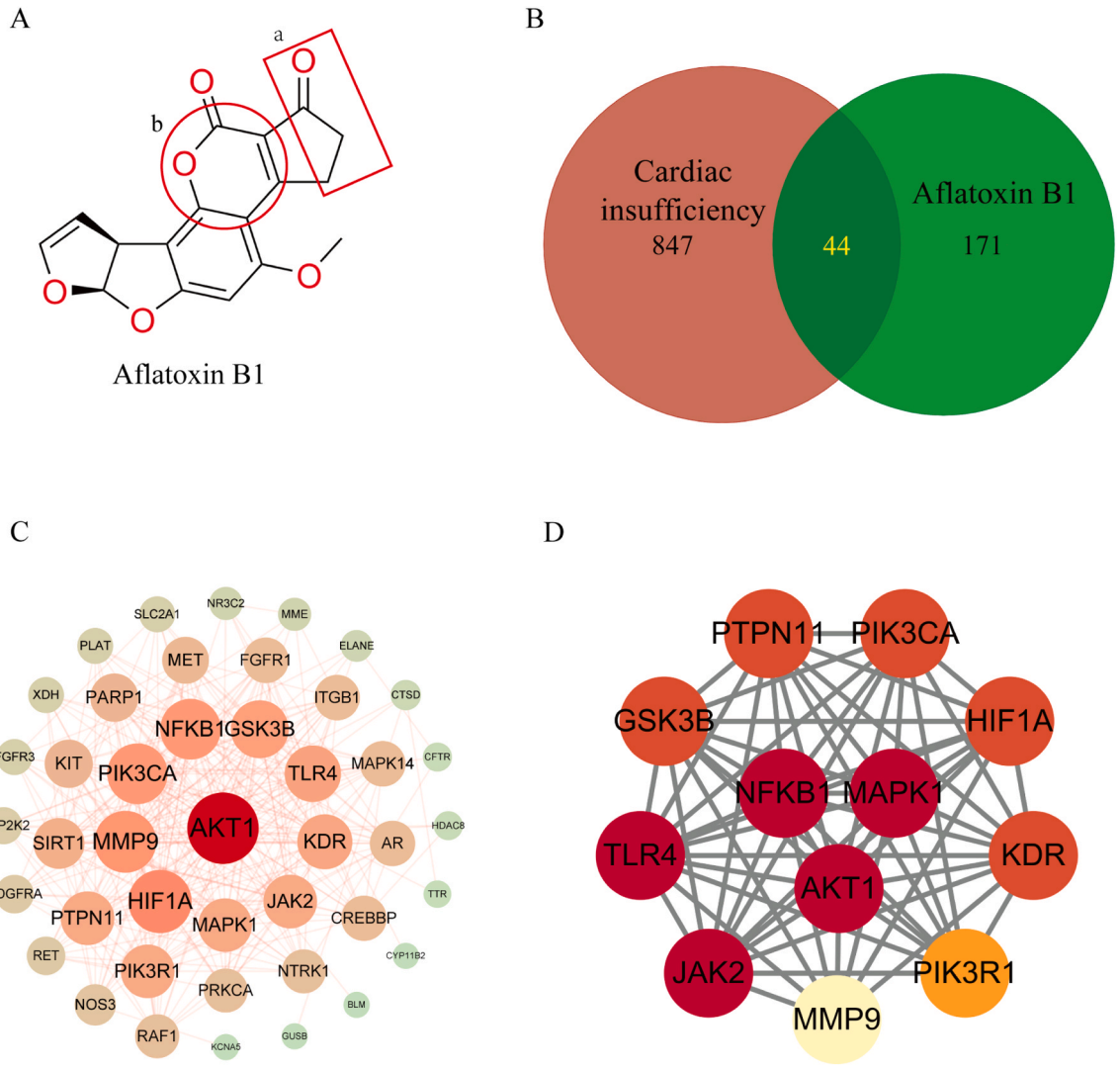

Fig. 1. AFB1-Related Targets Associated with Cardiac Insufficiency and PPI Network. (A) Schematic representation of the molecular structure of aflatoxin B1. Both red labels, a and b, indicate toxic regions of AFB1. (B) Venn diagram illustrating the overlap between AFB1-associated targets and cardiac insufficiency-related genes (n = 44). (C) PPI network of the 44 shared targets, constructed using the STRING database, depicting the functional relationships among genes linked to both AFB1 and cardiac insufficiency ($q<0.05$). Node color is mapped to degree centrality; redder nodes have higher degrees. (D) Topological analysis identified 12 core targets, highlighting key regulatory genes within the network. Node color is mapped to degree centrality; redder nodes have higher degrees.

PAGE), then transferred onto polyvinylidene difluoride membranes. Membranes were incubated with primary antibodies against AKT1 (Abiowell, Changsha, China), p-AKT1 (Abiowell, Changsha, China), MEK1/2 (Proteintech, Wuhan, China), p-MEK1/2 (Proteintech, Wuhan, China), and α-actin (Proteintech, Wuhan, China), followed by horseradish peroxidase-conjugated anti-mouse or anti-rabbit IgG secondary antibodies as appropriate.

3. Result

3.1. Identification of AFB1-related targets associated with cardiac insufficiency

AFB1 is commonly found in contaminated food and feed, particularly under warm and humid conditions (Fig. 1A). Using the SuperPred and Swiss Target Prediction platforms, 171 potential target genes for AFB1 were identified. In addition, 847 genes related to cardiac insufficiency were retrieved from the GeneCards and OMIM databases. Comparative analysis revealed 44 overlapping genes between the predicted AFB1 targets and the cardiac insufficiency-associated genes (Fig. 1B). These 44 intersecting targets imply a potential mechanistic link between AFB1 exposure and the development of cardiac insufficiency.

3.2. Construction and analysis of the PPI network associated with cardiac insufficiency

A PPI network was constructed from the 44 overlapping target genes using the STRING database (Fig. 1C). The network was further analyzed in Cytoscape, with hub genes identified by the CytoHubba plugin. This analysis revealed 12 core targets: AKT1, HIF1A, MMP9, PIK3CA, NFKB1, GSK3B, TLR4, KDR, JAK2, MAPK1, PIK3R1, and PTPN11. Visualization of these core genes is shown in Fig. 1D.

3.3. Enrichment analyses for GO and KEGG

GO and KEGG pathway enrichment analyses were conducted on the 44 potential target genes using RStudio. GO enrichment identified 2837 Biological Process (BP), 169 Cellular Component (CC), and 269 Molecular Function (MF) terms associated with these shared targets. For each category, the top ten terms-ranked by the number of enriched genes-were selected for visualization as bubble plots and bar charts (Fig. 2A, B). Specifically, BP terms were mainly related to the positive regulation of the MAPK cascade; CC terms were associated with membrane rafts and membrane microdomains; and MF terms were primarily enriched in protein tyrosine kinase activity.KEGG analysis revealed significant enrichment in 149 signaling pathways. The top 30 pathways, ranked by gene count, were illustrated using bubble plots and bar charts (Fig. 2C, D). Notably, the PI3K-AKT signaling pathway was identified as the core pathway through which AFB1 may contribute to cardiac insufficiency. In the PI3K-AKT pathway diagram (Fig. 2E), the overlapping genes between AFB1 targets and cardiac insufficiency-associated genes are highlighted in red.

3.4. Molecular docking of aflatoxin B1 with PI3K-AKT pathway-related targets

To elucidate the role of the PI3K-AKT signaling pathway in AFB1-induced cardiac insufficiency, we conducted molecular docking studies to examine the interactions between AFB1 and key pathway-related targets, including JAK2, GSK3B, HIF1A, AKT1, KDR, MAPK1, MAPK9, NFKB1, PIK3CA/PIK3R1, PTPN11, and TLR4 (Fig. 3A). The results revealed strong binding affinities between AFB1 and these core proteins, with binding energies below −5 kcal/mol, indicating favorable and spontaneous interactions. The docking conformations of the top four targets (based on binding energy) were visualized using PyMOL 2.3.0 (Fig. 3B-F), confirming robust AFB1 binding. These findings provide structural insights into how AFB1 may promote cardiac insufficiency through direct interactions with PI3K-AKT pathway components.

3.5. Evaluation of the effects of AFB1 on the molecular dynamics of the JAK2

To assess the molecular dynamics effects of AFB1 on JAK2, simulations were conducted using Gromacs 2024.4. The RMSD of the JAK2-AFB1 complex remained below 1 nm throughout the simulation, indicating high structural stability (Fig. 4A). The RMSF values also stayed below 1 nm, suggesting that AFB1 binding had minimal impact on the flexibility of JAK2 amino acid residues and preserved the structural integrity of the complex (Fig. 4B). The SASA remained consistently below 150 nm^2 (Fig. 4C), while the Rg fluctuated steadily around 2.0 nm (Fig. 4D). Collectively, these results demonstrate that binding of AFB1 does not induce significant structural perturbations in JAK2, supporting the stable formation of the JAK2-AFB1 complex.

The number of hydrogen bonds between JAK2 and AFB1 remained consistently at one with minimal fluctuation, indicating a stable and robust hydrogen bond interaction. Comparative analysis at five time points during the simulation (0, 25, 50, 75, and 100 ns) further confirmed the persistent binding stability, as AFB1 consistently occupied the same binding site on JAK2, with no significant positional shifts (Fig. 4E, F). Free energy landscape analysis, with RMSD, Rg, and Gibbs free energy set as the X, Y, and Z axes, respectively, revealed a single, well-defined energy minimum (Fig. 4G), providing further evidence for the conformational stability of the complex.

After system equilibration, the average binding free energy between JAK2 and AFB1 was calculated using the MM/GBSA method, yielding a value of -23.07 $kcal{\cdot}mol^{-1}$, indicative of strong binding affinity (Fig. 4H). Additionally, AFB1 formed stable interactions with the JAK2 residues LEU-983, LEU-855, and VAL-856, with binding energies of -2.35, -2.00, and -1.66 $kcal{\cdot}mol^{-1}$, respectively (Fig. 4I), identifying these residues as key contributors to ligand binding. These interactions were consistent with the initial molecular docking results, demonstrating that the binding pose remained stable throughout the simulation and further confirming the robustness of the JAK2-AFB1 complex.

3.6. AFB1 induces cardiac insufficiency and activates the PI3K-AKT and MAPK pathways

To further elucidate the mechanism by which AFB1 induces cardiac insufficiency, we established a mouse model of cardiac injury via intragastric gavage of AFB1. Cardiac injury and the extent of fibrosis were assessed using H&E and Masson staining (Fig. 5A). In the AFB1-treated group, myocardial tissue showed increased inflammatory cell infiltration, vacuolization of cardiomyocytes, and accumulation of collagen fibers between cardiomyocytes.

Transcriptional levels of several cardiac-specific markers were measured by qPCR. The results confirmed that AFB1-treated mice exhibited impaired cardiac function and increased collagen deposition (Fig. 5B-E). Consistent with the progression of cardiac insufficiency, inflammatory marker levels were also significantly elevated in the AFB1 group (Fig. 5F and G).

Based on network toxicology analyses and previous reports (Jiao et al., 2025), we hypothesized that AFB1 may promote cardiac insufficiency by activating the PI3K-AKT and MAPK signaling pathways. Prior studies have demonstrated that activation of these pathways exacerbates cardiac dysfunction. Notably, Western blot analysis showed that the total protein levels of AKT1 and MEK1/2 were only slightly increased in the AFB1 group, without statistical significance. However, the phosphorylation levels of p-AKT1 and p-MEK1/2 were significantly elevated (Fig. 5H and I). These results indicate that AFB1 activates the PI3K-AKT and MAPK pathways, contributing to the development of cardiac insufficiency.

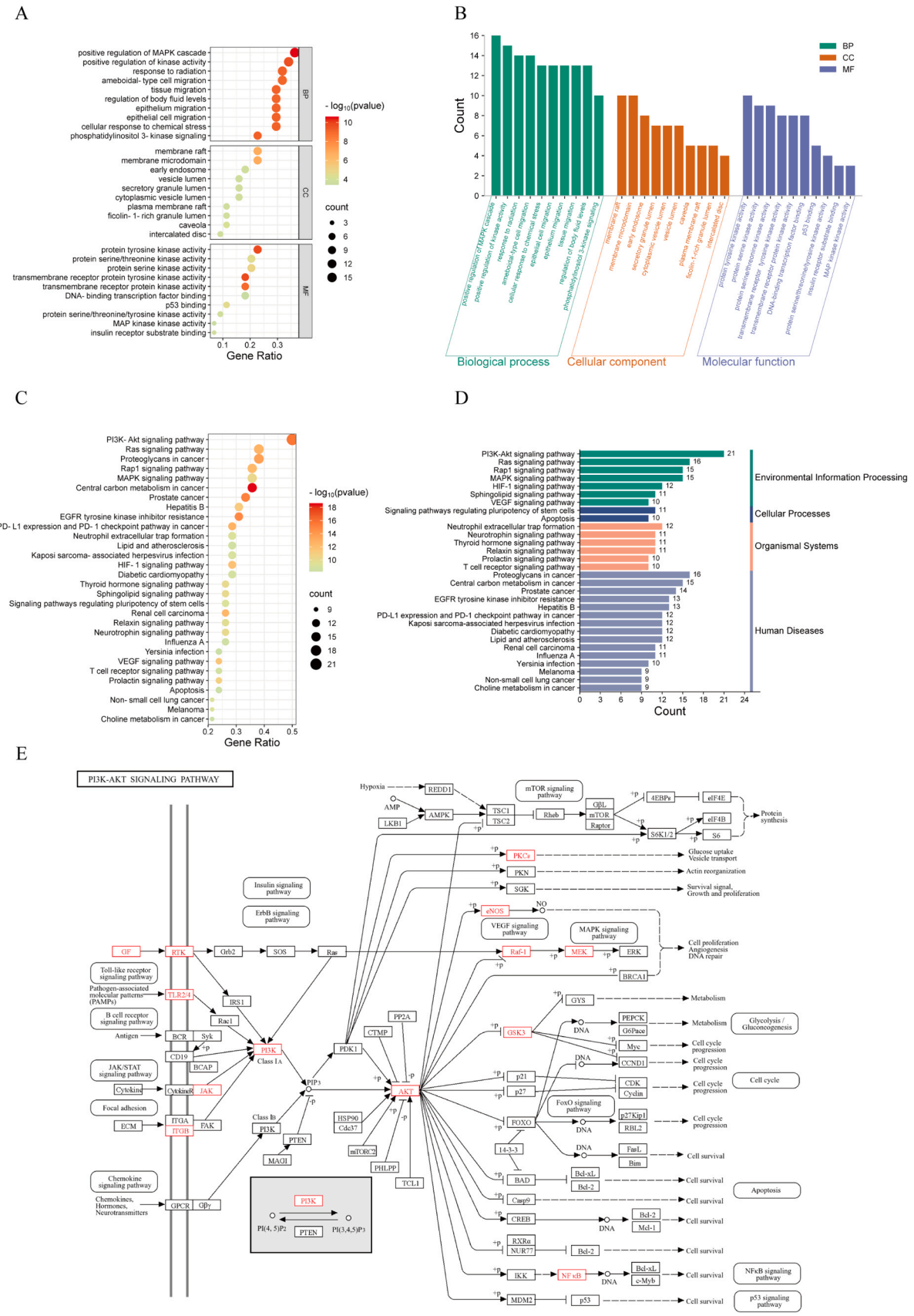

Fig. 2. Functional analysis of AFB1-associated targets. (A) GO analysis bubble plot (q<0.05); (B) GO analysis bar chart (q<0.05); (C) KEGG analysis bubble plot (q<0.05); (D) KEGG analysis bar chart (q<0.05); (E) KEGG pathway diagram, the red boxes represent genes enriched in the PI3K-AKT signaling pathway.

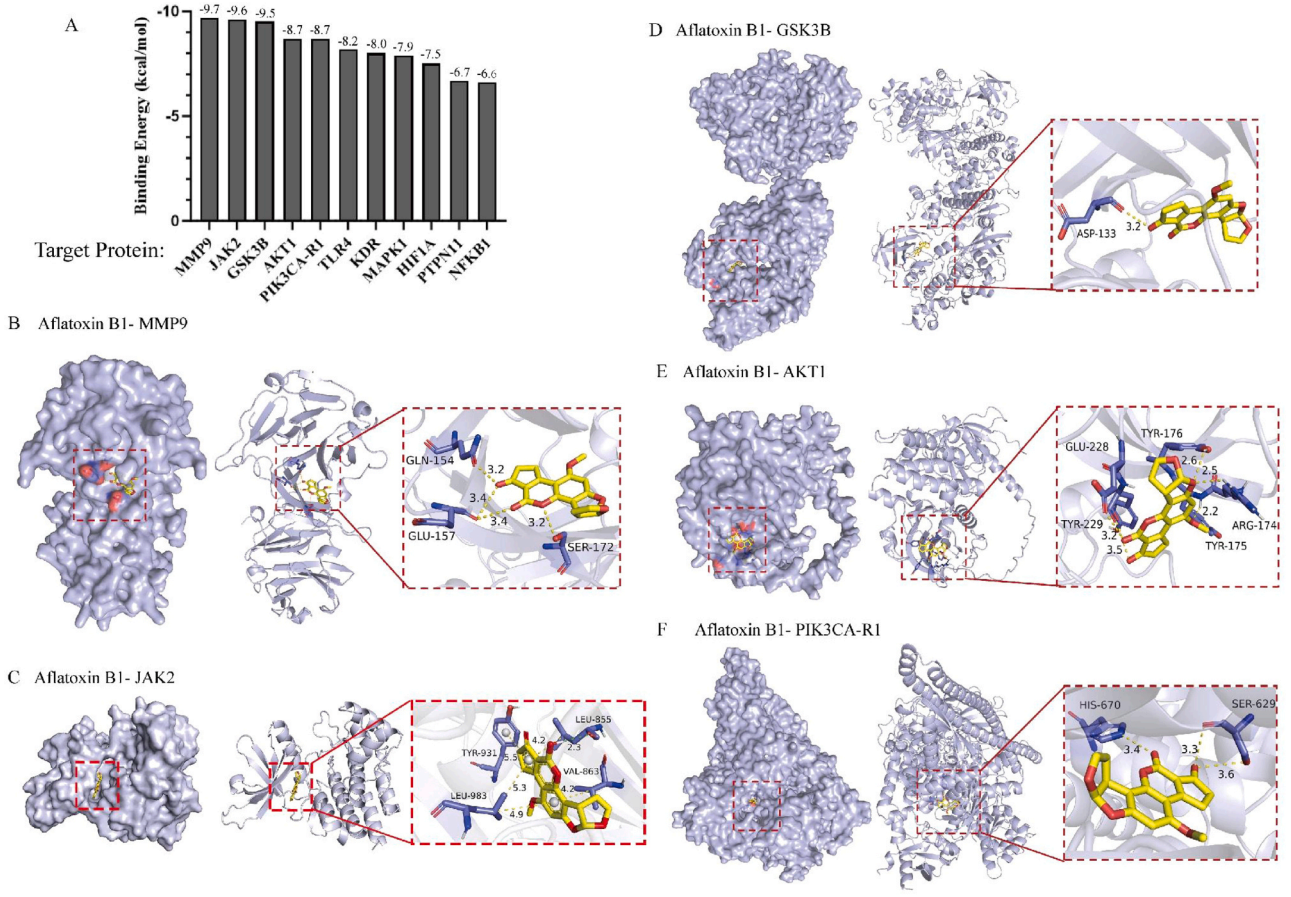

Fig. 3. Molecular docking simulations of AFB1 with PI3K-AKT pathway-related targets. (A) Summary of binding energies between AFB1 and the 11 target proteins in this pathway. (B) Molecular docking visualization of AFB1 with MMP9 protein. (C) Molecular docking visualization of AFB1 with JAK2 protein. (D) Molecular docking visualization of AFB1 with GSK3B protein. (E) Molecular docking visualization of AFB1 with AKT1 protein. (F) Molecular docking visualization of AFB1 with PI3KCA-R1 protein.

4. Discussion

AFB1 can be detected in various sources, including contaminated food, animal feed, medicinal herbs, and cereal crops, posing significant threats to public health and safety. Long-term exposure to AFB1 can lead to liver cancer, neurodegenerative diseases, and reproductive system disorders (Dai et al., 2024). The cardiotoxicity of AFB1 has garnered increasing attention, with research linking it to myocardial injury and inflammatory responses (Albadrani et al., 2024; Khalil et al., 2024). However, the effects and underlying mechanisms of chronic AFB1 exposure on cardiac insufficiency remain poorly understood. Therefore, further investigation into the impact of AFB1 on cardiac function and its molecular mechanisms is critically important.

We applied network toxicology to investigate the potential cardiotoxicity of AFB1 and identified overlapping targets associated with both AFB1 and cardiac insufficiency. Through this analysis, we screened 12 core targets, including AKT1, HIF1A, MMP9, PIK3CA, NFKB1, TLR4, KDR, JAK2, MAPK1, and PIK3R1, all of which are implicated in cardiac insufficiency. Molecular docking results showed that AFB1 had moderate binding affinity for NFKB1 but exhibited strong binding affinities for the other targets, suggesting that these interactions may contribute to the worsening of cardiac insufficiency. Subsequent enrichment analysis indicated significant activation of the PI3K-AKT and MAPK signaling pathways. Based on these findings, we focused on the roles of proteins within the PI3K-AKT and MAPK pathways in the context of AFB1-induced cardiac insufficiency.

The PI3K-AKT pathway is a critical cellular signaling cascade that regulates cell survival, proliferation, metabolism, and growth. This pathway plays a pivotal role in various diseases, and numerous studies have established a strong association between PI3K-AKT signaling and cardiac insufficiency. For instance, in aged mice, heightened activation of the PI3K-AKT-mTOR pathway results in reduced autophagy, ultimately leading to cardiac fibrosis (Qi et al., 2025). Similarly, activation of the PI3K-AKT-FoxO1 pathway has been observed in mouse models of cardiac insufficiency induced by transverse aortic constriction; inhibition of this pathway with Matairesinol significantly attenuated cardiac dysfunction (Zhang et al., 2024). In addition, Cytokinesis 2 has been shown to ameliorate post-myocardial infarction cardiac insufficiency and reduce myocardial fibrosis by suppressing PI3K-AKT pathway activity (Hu et al., 2024). Collectively, these findings indicate that activation of the PI3K-AKT pathway promotes the development of cardiac insufficiency. Therefore, we propose that AFB1 exacerbates cardiac insufficiency, at least in part, through activation of the PI3K-AKT signaling pathway.

MEK1/2 is a key component of the MAPK signaling pathway, transmitting signals from the upstream kinase Raf and activating downstream ERK1/2 through phosphorylation. Activated ERK1/2 primarily regulates cell proliferation and differentiation. Myocardial infarction is a major cause of cardiac insufficiency. Previous studies have shown that C1q/tumor necrosis factor-related protein 9 exacerbates cardiac insufficiency by upregulating Rap1 expression and activating MEK1/2 and ERK1/2 (Tan et al., 2025).Subsequently, inhibition of the MAPK and NF-κB pathways has been found to attenuate the AngII-induced inflammatory response in cardiac tissue and cardiomyocytes (Wang et al., 2025). These findings suggest that activation of the MAPK pathway promotes inflammation and the progression of

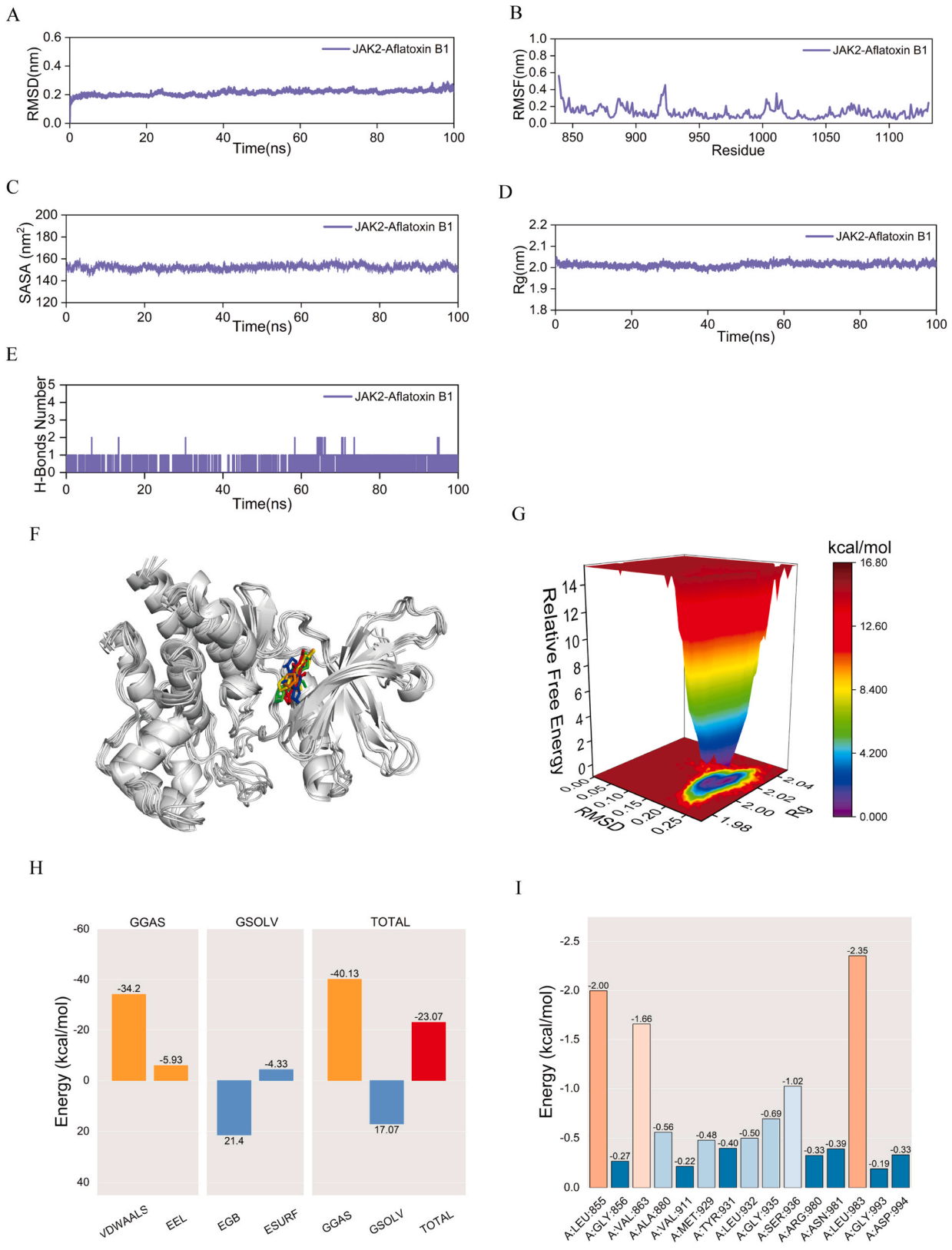

Fig. 4. Molecular dynamics simulation results. (A) Root mean square deviation (RMSD) curve, reflecting the degree of structural fluctuations within the complex. (B) Root mean square fluctuation (RMSF) curve, indicating the fluctuations of individual amino acid residues. (C) Solvent-Accessible Surface Area (SASA) curve, reflecting the degree of protein folding and bending. (D) Radius of gyration (Rg) curve, indicating the degree of expansion of the complex system. (E) Hydrogen bond analysis, showing the hydrogen bonding properties at the binding sites of the complex. (F) Comparative structural analysis of the complex at five time points (0, 25, 50, 75, and 100 nanoseconds) during the molecular dynamics simulation. (G) Free energy landscape, where the concentration of energy clusters reflects the stability of the complex state. (H) Average binding free energy, representing the binding strength between AFB1 and JAK2. (I) Energy contributions of amino acid residues involved in ligand binding, indicating their degree of contribution to the binding process.

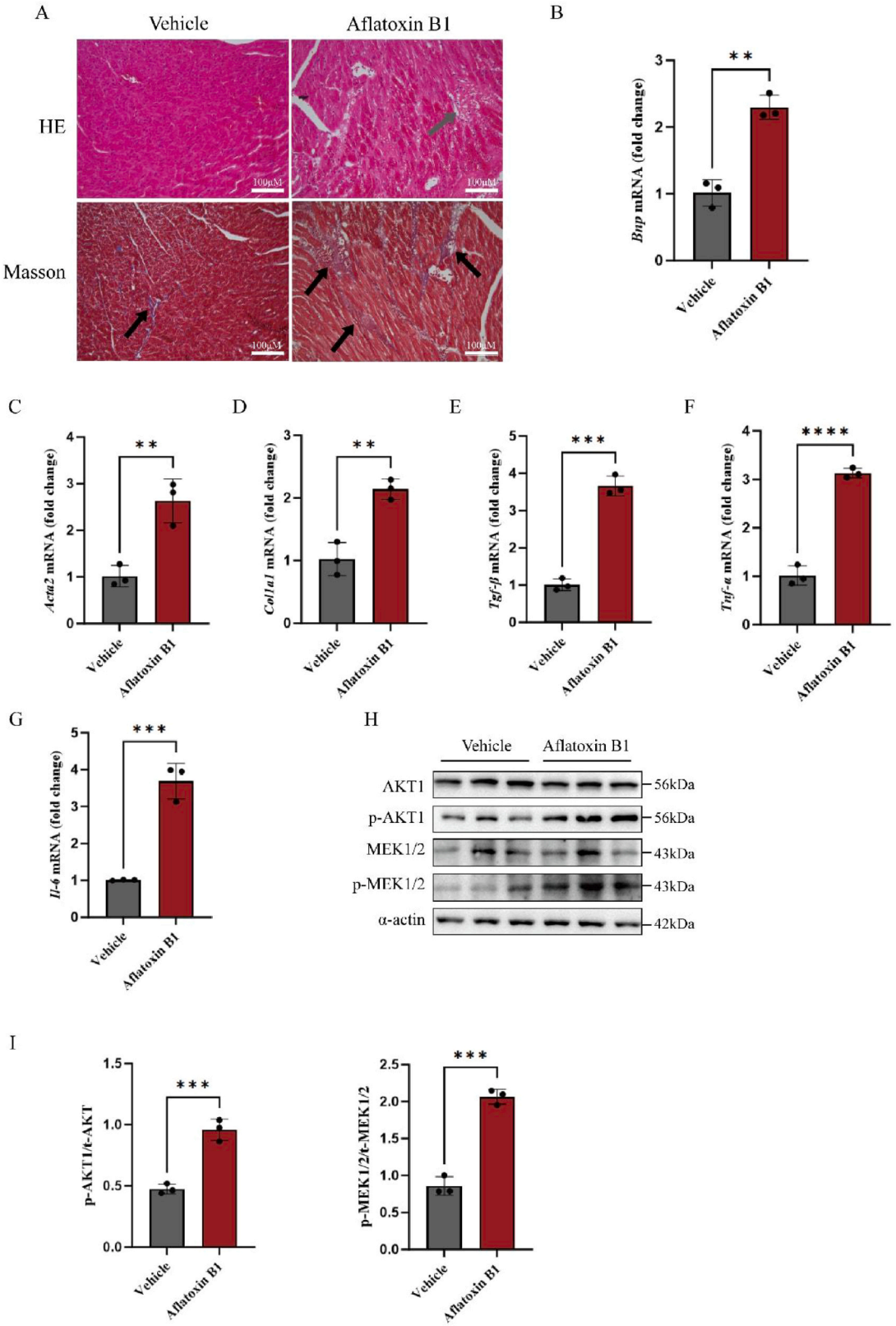

Fig. 5. AFB1 activates the PI3K-AKT and MAPK pathways, leading to cardiac fibrosis and impaired cardiac function. (A) Representative H&E and Masson's trichrome staining of left ventricular sections from mice in the vehicle group and the AFB1-treated group (n = 3).Gray arrows denote inflammatory cell infiltration in myocardial tissue; black arrows denote myocardial fibrosis. (B-G) qPCR analysis of the transcriptional levels of the heart failure marker (BNP), cardiac fibrosis markers (Acta2, COL1A1, and TGF-β), and inflammatory markers (IL-6 and TNF-α) in cardiac tissue (n = 3). (H and I) Western blot analysis shows the expression levels of AKT1, p-AKT1, MEK1/2, and p-MEK1/2 in cardiac tissue, with α-actin as loading control (n = 3). Compared with the vehicle group: ***$p < 0.001$; **$p < 0.01$; *$p < 0.05$;ns > 0.05.

cardiac insufficiency. Therefore, by activating the MAPK signaling pathway, AFB1 may exacerbate cardiac inflammation and accelerate the development of cardiac insufficiency.

KEGG pathway analysis revealed that JAK2 is positioned upstream of the PI3K-AKT signaling cascade and subsequently activates downstream pathways. Molecular docking studies indicated that AFB1 binds to JAK2 with a binding free energy of -9.6 kcal·mol^{-1} . Additionally, molecular dynamics simulations demonstrated high stability of the JAK2-AFB1 complex across multiple metrics, including RMSD, RMSF, radius of gyration, number of hydrogen bonds, and the distribution of binding free energy.

Based on the above analysis, we propose that AFB1 may bind to JAK2 and further activate the PI3K-AKT and MAPK signaling pathways, thereby promoting the development of cardiac insufficiency. Our integrated approach—utilizing network pharmacology, molecular docking, and molecular dynamics simulations—provided predictive insights into the interactions between AFB1 and key proteins. However, these computational models have inherent limitations and cannot fully replicate the complexity of biological systems in vivo.

To address this, we established a mouse model of AFB1-induced cardiac insufficiency. In vivo experiments confirmed that long-term exposure to AFB1 in mice exacerbated cardiac fibrosis and significantly increased inflammatory markers. Moreover, Western blot analysis demonstrated that AFB1 elevated the phosphorylation levels of AKT1 and MEK1/2, indicating activation of both the AKT and MEK signaling pathways.

This study combined network toxicology simulations with in vivo experimental validation to comprehensively elucidate the impact of AFB1 on cardiac insufficiency and its underlying mechanisms. Our findings offer valuable insights for developing more effective strategies to evaluate the toxicity of environmental pollutants, and provide a scientific basis for shaping regulatory policies and promoting the rational use of antimicrobial agents. In subsequent research, we will investigate dose-dependent cardiac effects of AFB1 and determine whether liver injury mediates secondary impacts on cardiac function. Moreover, we will delve into the mechanisms underlying AFB1-induced cardiac alterations and identify candidate drugs capable of attenuating its cardiotoxicity.

5. Conclusion

In this study, we integrated network toxicology, molecular docking, molecular dynamics simulations, and in vivo mouse experiments to thoroughly assess the potential impact of AFB1 on cardiac insufficiency. We identified 44 overlapping targets associated with both AFB1 exposure and cardiac insufficiency, from which 12 core targets were further screened, suggesting that AFB1 may aggravate cardiac insufficiency by modulating these key proteins. Enrichment analysis revealed significant associations with the positive regulation of the MAPK cascade, membrane raft components, and protein tyrosine kinase activity, highlighting the PI3K-AKT signaling pathway as a primary mechanism involved.

Molecular docking of AFB1 with the 12 core targets demonstrated that these proteins play critical roles in the progression of AFB1-induced cardiac insufficiency. JAK2, an upstream regulator of the PI3K-AKT pathway, was selected for molecular dynamics simulations, which revealed a highly stable JAK2–AFB1 complex. These findings indicate that AFB1 may promote cardiac insufficiency by binding to JAK2 and subsequently activating the PI3K-AKT and MAPK pathways.

To validate these computational predictions, we performed in vivo experiments in mice. The results confirmed and extended our simulation findings, providing comprehensive insight into the core targets and molecular mechanisms by which AFB1 exposure induces cardiac insufficiency. Collectively, this study offers a theoretical foundation for developing interventions to mitigate AFB1-induced cardiac dysfunction.

Funding

Our study was supported by Liaoning Province Science and Technology Joint Program (Applied basic research project) (2023JH2/101700199) and Liaoning Province Science and Technology Joint Program (General Program) (2023-MSLH-293).

CRediT authorship contribution statement

Zhonghua Wen: Formal analysis. **Yangyang Liu:** Writing – review & editing, Methodology. **Qian Cao:** Writing – review & editing, Project administration. **Siyao Wang:** Writing – review & editing, Supervision, Project administration. **Xiaotong Zhao:** Data curation. **Qing Zhang:** Writing – original draft, Software, Data curation. **Piqiao Jiang:** Formal analysis. **Qianyao Zhang:** Writing – original draft, Visualization, Methodology, Data curation.

Declaration of Competing Interest

The authors declare that they have no known competing financial interests or personal relationships that could have appeared to influence the work reported in this paper.

Data availability

Data will be made available on request.

References

Albadrani, G.M., Altyar, A.E., Kensara, O.A., Haridy, M.A.M., Zaazouee, M.S., Elshanbary, A.A., Sayed, A.A., Abdel-Daim, M.M., 2024. Antioxidant, anti-inflammatory, and anti-DNA damage effects of carnosic acid against aflatoxin B1-induced hepatic, renal, and cardiac toxicities in rats. Toxicol. Res (Camb.) 13 (3), tfae083. https://doi.org/10.1093/toxres/tfae083.

Altyar, A.E., Kensara, O.A., Sayed, A.A., Aleya, L., Almutairi, M.H., Zaazouee, M.S., Elshanbary, A.A., El-Demerdash, F.M., Abdel-Daim, M.M., 2023. Acute aflatoxin B1-induced hepatic and cardiac oxidative damage in rats: ameliorative effects of morin. Heliyon 9 (11). https://doi.org/10.1016/j.heliyon.2023.e21837.

Cao, W., Yu, P., Yang, K., Cao, D., 2022. Aflatoxin B1: metabolism, toxicology, and its involvement in oxidative stress and cancer development. Toxicol. Mech. Methods 32 (6), 395–419. https://doi.org/10.1080/15376516.2021.2021339.

Chen, K.J., Zhang, Y., Zhu, X.Y., Yu, S., Xie, Y., Jin, C.J., Shen, Y.M., Zhou, S.Y., Dai, X.C., Su, S.A., Xie, L., Huang, Z.X., Gong, H., Xiang, M.X., Ma, H., 2025. GSTM1 suppresses cardiac fibrosis post-myocardial infarction through inhibiting lipid peroxidation and ferroptosis. Mil. Med Res 12 (1), 26. https://doi.org/10.1186/s40779-025-00610-6.

Claeys, L., Romano, C., De Ruyck, K., Wilson, H., Fervers, B., Korenjak, M., Zavadil, J., Gunter, M.J., De Saeger, S., De Boevre, M., Huybrechts, I., 2020. Mycotoxin exposure and human cancer risk: a systematic review of epidemiological studies. Compr. Rev. Food Sci. Food Saf. 19 (4), 1449–1464. https://doi.org/10.1111/1541-4337.12567.

Dai, C., Tian, E., Hao, Z., Tang, S., Wang, Z., Sharma, G., Jiang, H., Shen, J., 2022. Aflatoxin B1 toxicity and protective effects of curcumin: molecular mechanisms and clinical implications. Antioxid. (Basel) 11 (10). https://doi.org/10.3390/antiox11102031.

Dai, C., Sharma, G., Liu, G., Shen, J., Shao, B., Hao, Z., 2024. Therapeutic detoxification of quercetin for aflatoxin B1-related toxicity: roles of oxidative stress, inflammation, and metabolic enzymes. Environ. Pollut. 345, 123474. https://doi.org/10.1016/j.envpol.2024.123474.

van den Borne, S.W., Diez, J., Blankesteijn, W.M., Verjans, J., Hofstra, L., Narula, J., 2010. Myocardial remodeling after infarction: the role of myofibroblasts. Nat. Rev. Cardiol. 7 (1), 30–37. https://doi.org/10.1038/nrcardio.2009.199.

Ge, J., Yu, H., Li, J., Lian, Z., Zhang, H., Fang, H., Qian, L., 2017. Assessment of aflatoxin B1 myocardial toxicity in rats: mitochondrial damage and cellular apoptosis in cardiomyocytes induced by aflatoxin B1. J. Int. Med. Res. 45 (3), 1015–1023. https://doi.org/10.1177/0300060517706579.

Hu, G., Chen, J., Chen, M., Yang, K., Wang, Y., Ma, Z., Bao, H., Ding, X., 2024. Silencing DOCK2 attenuates cardiac fibrosis following myocardial infarction in mice via targeting PI3K/Akt and Wnt/beta-Catenin pathways. J. Cardiovasc Transl. Res 17 (6), 1442–1454. https://doi.org/10.1007/s12265-024-10533-7.

Jiao, R., Li, W., Gu, X., Liu, J., Liu, Z., Hu, Y., Yang, Z., Liu, Y., Liu, X., Gu, R., Li, L., Li, X., 2025. Lenalidomide attenuates cardiac fibrosis and inflammation induced by beta-adrenergic receptor activation. Int Immunopharmacol. 158, 114848. https://doi.org/10.1016/j.intimp.2025.114848.

Khalil, H.M.A., Eid, W.A.M., El-Nablaway, M., El Nashar, E.M., Al-Tarish, J.S., El Henafy, H.M.A., 2024. Date seeds powder alleviate the aflatoxin B1 provoked heart toxicity in Male offspring rat. Sci. Rep. 14 (1), 30480. https://doi.org/10.1038/s41598-024-80197-5.

Meijer, N., Stoopen, G., van der Fels-Klerx, H.J., van Loon, J.J.A., Carney, J., Bosch, G., 2019. Aflatoxin B(1) conversion by black soldier Fly (Hermetia illucens) larval enzyme extracts. Toxins (Basel) 11 (9). https://doi.org/10.3390/toxins11090532.

Qi, J., Lu, B., Jin, C.W., Shang, Y.Y., Pan, H., Li, H., Tong, Z.J., Zhang, W., Han, L., Zhong, M., 2025. FP receptor inhibits autophagy to aggravate aging-related cardiac fibrosis through PI3K/AKT/mTOR signaling pathway. Arch. Gerontol. Geriatr. 133, 105824. https://doi.org/10.1016/j.archger.2025.105824.

Ranjbar, S., Mohammadi, P., Pashaei, S., Sadeghi, M., Mehrabi, M., Shabani, S., Ebrahimi, A., Bruhl, A.B., Khodarahmi, R., Brand, S., 2025. Effect of aflatoxin B1 on the nervous system: a systematic review and network analysis highlighting alzheimer's disease. Biol. (Basel) 14 (4). https://doi.org/10.3390/biology14040436.

Rushing, B.R., Selim, M.I., 2019. Aflatoxin B1: a review on metabolism, toxicity, occurrence in food, occupational exposure, and detoxification methods. Food Chem. Toxicol. 124, 81–100. https://doi.org/10.1016/j.fct.2018.11.047.

Sabahi, M., Karimipour, M., Ahmadi, A., Pourheydar, B., Farjah, G., 2024. The protective effects of melatonin on testis, sperm parameters quality, and in-vitro fertilization in mice following treatment with aflatoxin B1: an experimental study. Int J. Reprod. Biomed. 23 (2), 185–198. https://doi.org/10.18502/ijrm.v23i2.18492.

Tan, Y., Li, H., Cao, G., Xin, J., Yan, D., Liu, Y., Li, P., Zhang, Y., Shi, L., Zhang, B., Yi, W., Sun, Y., 2025. N-terminal domain of CTRP9 promotes cardiac fibroblast activation in myocardial infarction via Rap1/Mek/Erk pathway. J. Transl. Med. 23 (1). https://doi.org/10.1186/s12967-025-06274-z.

Wang, Y., Zhang, R., Li, J., Guo, S., Yuan, Y., Zheng, R., Xu, Y., Cai, X., 2025. Tetrandrine improves ventricular remodeling and inflammation via inhibition of the MAPK/NF-κB pathway. Int. Heart J. 66 (3), 463–474. https://doi.org/10.1536/ihj.24-697.

Yan, Y.C., Dong, P.Y., Ma, H.H., Chen, Y., Bai, Y., Li, Y.Y., Dong, Y., Shen, W., Zhang, X. F., 2025. Vitamin B6 alleviates aflatoxin B1-Induced impairment of testis development by activating the PI3K/Akt signaling pathway. J. Agric. Food Chem. 73 (6), 3724–3736. https://doi.org/10.1021/acs.jafc.4c10966.

Zhang, T., Li, L., Mo, X., Xie, S., Liu, S., Zhao, N., Zhang, H., Chen, S., Zeng, X., Wang, S., Deng, W., Tang, Q., 2024. Matairesinol blunts adverse cardiac remodeling and heart failure induced by pressure overload by regulating Prdx1 and PI3K/AKT/FOXO1 signaling. Phytomedicine 135, 156054. https://doi.org/10.1016/j.phymed.2024.156054.

Zhou, X., Gan, F., Hou, L., Liu, Z., Su, J., Lin, Z., Le, G., Huang, K., 2019. Aflatoxin B(1) induces immunotoxicity through the DNA Methyltransferase-Mediated JAK2/STAT3 pathway in 3D4/21 cells. J. Agric. Food Chem. 67 (13), 3772–3780. https://doi.org/10.1021/acs.jafc.8b07309.